Computing Time-Periodic Solutions of a Model for the Vortex Sheet with Surface Tension

David M. Ambrose*† Mark Kondrla, Jr.* Michael Valle*

October 8, 2012

Abstract

We compute time-periodic solutions of a simple model for the vortex sheet with surface tension. The model has the same dispersion relation as the full system of evolution equations, and also has the same destabilizing nonlinearity (if the surface tension parameter were to be set to zero, then this nonlinearity would cause an analogue of the Kelvin-Helmholtz instability). The numerical method uses a gradient descent algorithm to minimize a functional which measures whether a solution of the system is time-periodic. We find continua of genuinely time-periodic solutions bifurcating from equilibrium.

Keywords: vortex sheet, surface tension, time-periodic, gradient descent

1 Introduction

We compute time-periodic solutions of a model for the vortex sheet with surface tension. A vortex sheet is an interface between two different fluids, across which there is a jump in the tangential components of the fluids' velocities. The full equations of motion for the vortex sheet are given by the incompressible Euler equations. In the case of irrotational flow, a boundary integral formulation may be used, and these equations can be studied by considering only quantities defined along the interface, thus reducing the dimension of the problem by one.

The surface tension force is highly singular, in that it is present only at the interface between the two fluids, and in that the surface tension coefficient arises in the evolution equations as being multiplied by the curvature of the interface. The curvature is nonlinear and includes second derivatives of the parameterization of the interface, leading to difficulties in both analysis and computing if the interface is described using its Cartesian coordinates. A breakthrough in the computing of this system was achieved by Hou, Lowengrub, and Shelley when the problem was formulated instead using geometric quantities (the tangent angle and the arclength element) which are naturally related to the curvature [14, 13]. This formulation was subsequently used to show that the initial value problem for the system is well-posed [1].

Despite these breakthroughs, there are still many difficult questions to address for the vortex sheet with surface tension. One such question is whether certain singularities, known as Moore singularities, can form in the vortex sheet with surface tension [17]. In such a singularity, the curvature of the interface would become infinite for at least one point. Such singularities are known to exist when surface tension effects are negligible [16, 20], but there is disagreement in the literature as to whether these singularities occur when the surface tension is nontrivial [12, 21].

*Department of Mathematics, Drexel University, 3141 Chestnut St., Philadelphia, PA 19104. We gratefully acknowledge support from the National Science Foundation through NSF grants DMS-1008387 and DMS-1016267. We also gratefully acknowledge support in the form of Research Co-Op Funding from the Drexel University Office of the Provost and the Steinbright Career Development Office.

†Corresponding author.

To study this question of the existence of Moore singularities for the vortex sheet with surface tension, a simple model was introduced [2]. The model is formed by first writing the evolution equations in the tangent-angle/arclength formulation as in the Hou, Lowengrub, and Shelley work, and then neglecting all but the leading-order, linear terms as well as the leading-order nonlinear term. The terms which are retained are the only terms which contribute to the dispersion relation for the system, so the simplified model has the same dispersion relation as the full system. Furthermore, the model retains a version of the Kelvin-Helmholtz instability that the vortex sheet without surface tension is known for, owing to the structure of the leading-order nonlinear term. A numerical study was made using this simplified model in [2], and it was found that the curvature of the interface could become infinite at isolated points.

Another open question for the full vortex sheet with surface tension is the existence of time-periodic solutions. Such solutions are known to exist for some systems in interfacial fluid dynamics, such as the Benjamin-Ono equation or the irrotational water wave [5], [19], [15]. For the vortex sheet with surface tension, while there is not yet a proof of existence of time-periodic solutions, there has been a computational study [4]. A proof of existence of such waves for the full system of equations of motion for the vortex sheet with surface tension would be quite difficult, and it seems prudent to attempt first a proof using the simple model. However, it is helpful to first repeat the computations of time-periodic solutions for the model system to gather evidence of the existence of such waves for the model. This is the subject of the present work: a computational investigation of the existence of families of time-periodic solutions of the simple model for the vortex sheet with surface tension.

The numerical method used is a simplified version of the method used for the full vortex sheet problem. This method was first developed to study time-periodic solutions of the Benjamin-Ono equation [5], [3]. The essential steps of the method are to first define a functional which measures whether a solution of the initial value problem is in fact a time-periodic solution, for a given period. Then, the variational derivative of the functional with respect to the inital data and the presumed period is computed analytically. It turns out that the variational derivative is the solution to a different evolutionary partial differential equation. We minimize this functional numerically, using a gradient descent algorithm (the Broyden-Fletcher-Goldfarb-Shanno, or BFGS, algorithm) [18]. For the initial guess for the BFGS algorithm, at least at small amplitude, we use a time-periodic solution of the linearization of the model equations about the zero equilibrium.

The computational study of the full system found a continuum of solutions bifurcating from the zero equilibrium. We find the same for the simplified model. This helps to validate the model, showing that many of the essential dynamics of the system are captured by retaining only the leading-order, linear (dispersive) terms, as well as the cubic, destabilizing nonlinearity. Furthermore, these findings indicate that it may be possible to construct a proof of the existence of time-periodic solutions for the model. The proof would most likely proceed using the so-called Craig-Wayne-Bourgain method, in which a version of the Nash-Moser implicit function theorem is applied [11, 9, 8]. The conclusion of the proof would be that there exists a family of time-periodic solutions in a neighborhood of the zero equilibrium.

In addition to the Benjamin-Ono equation and the vortex sheet with surface tension, a version of the numerical method for finding time-periodic solutions has also been applied to the irrotational two-dimensional water wave [22]. We note that all three of these problems are Hamiltonian; see the references [10], [7], [23] for details of the Hamiltonian description in each case. The model we study at present was not constructed in order to maintain a Hamiltonian structure; in fact, other than the mean values of the dependent variables, we expect that there are no conserved quantities. Nevertheless, we still find many time-periodic solutions, demonstrating that Hamiltonian structure is in no way necessary for the success of the numerical method.

In addition to validating the model and finding evidence to support future analytical directions, we also find some solutions which were not previously studied for the full system: non-symmetric solutions. We are able to find these solutions because we use a simplified version of the algorithm, requiring less knowledge of the solutions ahead of time. The algorithm used for the full problem reduced the necessary computations to one-quarter of one period of the time-periodic solutions, by studying only solutions for which the full behavior can be deduced from the solution over a quarter period. We instead allow for more general behaviors, by computing over the full period of the solution. For our inital guess in the BFGS algorithm, we choose time-periodic solutions of the linearized equations which lack both even and odd symmetry. The algorithm then

converges to time-periodic solutions of the simple model which also lack these symmetries.

The plan of the paper is as follows: in Section 2, we give the equations of motion for the vortex sheet with surface tension and for the simplified model. We also discuss the well-posedness of the initial value problem for the model. In Section 3, we give details of the numerical method for computing time-periodic solutions. In Section 4, we give formulas for time-periodic solutions of the linearized equations of motion. In Section 5, we give the results of the computations. We make some concluding remarks in Section 6.

2 The model

In this section, we first describe the full equations of motion for the vortex sheet with surface tension. Then, we describe the approximations that we make, resulting in the model. As we have said, this model was originally developed in [2].

A vortex sheet is an interface between two inviscid, irrotational, incompressible fluids, across which this is a jump in the tangential components of the fluid velocities. We consider the case in which the fluids are two-dimensional, and of infinite vertical extent, and horizontally periodic. Furthermore, we consider the density-matched case. Since the fluids are two-dimensional, the interface between them is one-dimensional. We let $(x(\alpha,t),y(\alpha,t))$ be the parameterization of the curve; here, t is time and α is the spatial parameter along the curve. We let s_α be the arclength element, so that $s_\alpha^2 = x_\alpha^2 + y_\alpha^2$. Then, we define unit tangent and normal vectors at each point along the curve as $\hat{\mathbf{t}} = (x_\alpha, y_\alpha)/s_\alpha$ and $\hat{\mathbf{n}} = (-y_\alpha, x_\alpha)/s_\alpha$, respectively. Since the curve is horizontally periodic, we have $x(\alpha+2\pi,t) = x(\alpha,t) + 2\pi$ and $y(\alpha+2\pi,t) = y(\alpha,t)$, for all α and t.

We can describe the motion of the vortex sheet as

$$(x,y)_t = U\hat{\mathbf{n}} + V\hat{\mathbf{t}}.$$

The normal velocity, U, is determined by the fluid dynamics. The tangential velocity, V, can be chosen according to our preference as to a parameterization of the curve. That is, if α were to be, for instance, a Langrangian variable, then V would be chosen in a particular way. We choose α to be a (normalized) arclength parameter, and so this determines V. In particular, if $\theta = \arctan(y_\alpha/x_\alpha)$ is the tangent angle the curve forms with the horizontal, then we find $s_{\alpha t} = V_\alpha - \theta_\alpha U$. If L is the length of one period of the curve, $L = \int_0^{2\pi} s_\alpha \, d\alpha$, then we want $s_{\alpha t} = L_t/2\pi$. This implies $V_\alpha = \theta_\alpha U + L_t/2\pi$, and this can be integrated to give a formula for V in terms of the position of the curve and U. Instead of evolving x and y, the Cartesian coordinates of the curve, it is shown in [14], [13], and [1] that evolving θ is helpful; the evolution equation for θ is

$$\theta_t = \frac{U_\alpha + V\theta_\alpha}{s_\alpha}.$$

We now give the definition of U. As we said, U is determined by the fluid dynamics. The particular fluid dynamics that we are considering are that each fluid is irrotational in the bulk, but there is a jump in the tangential velocity across the interface. Therefore, taking the curl of the velocity, we get a Dirac mass supported at the interface. That is, the vorticity is $\omega = \gamma(\alpha,t)\delta_{\mathcal{C}}$, where $\delta_{\mathcal{C}}$ is the Dirac mass of the curve $\mathcal{C} = (x,y)$. The fluid velocity can be recovered from the vorticity by using the Biot-Savart law as usual; then, taking the limit of the velocity approaching the free surface, we find $U = \mathbf{W}\cdot\hat{\mathbf{n}}$, where the Birkhoff-Rott integral, $\mathbf{W} = (W_1, W_2)$, is given by

$$W_1(\alpha,t) - iW_2(\alpha,t) = \frac{1}{4\pi}\mathrm{PV}\int_0^{2\pi} \gamma(\alpha',t)\cot\left(\frac{(x(\alpha)-x(\alpha')) + i(y(\alpha)-y(\alpha'))}{2}\right)\, d\alpha'.$$

To finish describing the equations of motion for the vortex sheet with surface tension, we must give the evolution equation for γ. Using the arclength parameterization, we have

$$\gamma_t = \tau\frac{\theta_{\alpha\alpha}}{s_\alpha} + \frac{\left((V - \mathbf{W}\cdot\hat{\mathbf{t}})\gamma\right)_\alpha}{s_\alpha},$$

where $\tau > 0$ is the constant coefficient of surface tension; note that there would be additional terms in the γ_t equation if we allowed the two fluids to have different densities.

We substitute the definition of U into the evolution equation for θ, and we also expand the derivative in the evolution equation for γ; this requires the elementary geometric formulas $\hat{\mathbf{t}}_\alpha = \theta_\alpha \hat{\mathbf{n}}$ and $\hat{\mathbf{n}}_\alpha = -\theta_\alpha \hat{\mathbf{t}}$. We get the following:

$$\theta_t = \frac{\mathbf{W}_\alpha \cdot \hat{\mathbf{n}} + (V - \mathbf{W} \cdot \hat{\mathbf{t}})\theta_\alpha}{s_\alpha}, \qquad \gamma_t = \tau \frac{\theta_{\alpha\alpha}}{s_\alpha} + \frac{(\mathbf{W}_\alpha \cdot \hat{\mathbf{t}})\gamma}{s_\alpha} + \frac{s_{\alpha t}\gamma}{s_\alpha} + \frac{(V - \mathbf{W} \cdot \hat{\mathbf{t}})\gamma_\alpha}{s_\alpha}.$$

We introduce the notation $f \sim g$, as used in [13], to indicate that $f - g$ is smoother than either f or g. Then, using the first-order Taylor formulas, $x(\alpha) - x(\alpha') \approx x_\alpha(\alpha')(\alpha - \alpha')$ and $y(\alpha) - y(\alpha') \approx y_\alpha(\alpha')(\alpha - \alpha')$, the first author proved the following formulas in [1]:

$$\mathbf{W}_\alpha \cdot \hat{\mathbf{n}} \sim \frac{1}{2s_\alpha} H(\gamma_\alpha), \qquad \mathbf{W}_\alpha \cdot \hat{\mathbf{t}} \sim \frac{1}{2s_\alpha} H(\gamma\theta_\alpha),$$

where H is the Hilbert transform. Using this approximation, we have

$$\left(\mathbf{W}_\alpha \cdot \hat{\mathbf{t}}\right)\gamma \sim \frac{1}{2s_\alpha}\gamma H(\gamma\theta_\alpha).$$

We also have that the commutator of the Hilbert transform and multiplication by a smooth function is smoothing; therefore we have

$$\left(\mathbf{W}_\alpha \cdot \hat{\mathbf{t}}\right)\gamma \sim \frac{1}{2s_\alpha}\gamma^2 H(\theta_\alpha).$$

Now, we form our model. We use these approximations, and we also drop the transport terms (that is, we drop the terms $(V - \mathbf{W} \cdot \hat{\mathbf{t}})\theta_\alpha / s_\alpha$ and $(V - \mathbf{W} \cdot \hat{\mathbf{t}})\gamma_\alpha / s_\alpha$). Furthermore, we drop factors of s_α, and for simplicity, we also ignore factors of 2. Finally, we mention that the average value of γ is conserved, and we want the corresponding quantity to be conserved in the model. Based on all of these considerations, our model is:

$$u_t = H(v_x), \qquad v_t = \tau u_{xx} + \mathbb{P}\left(v^2 H(u_x)\right). \tag{1}$$

We have said that the nonlinearity is destabilizing, and we remark that the destabilizing nature of the nonlinearity can be clearly seen from the linearization of the system, as in equation (9) below. The system (1) is taken together with the initial conditions

$$u(x,0) = u_0(x), \qquad v(x,0) = v_0(x). \tag{2}$$

Here, u is meant to stand in for θ and v is meant to stand in for γ. Since we no longer have the presence of the arclength in the model, we have changed notation for the independent variable from α to x. The operator $\mathbb{P}$ is projection off the mean; that is, if f is any 2π-periodic function, then

$$\mathbb{P}f = f - \frac{1}{2\pi}\int_0^{2\pi} f(x')\, dx'.$$

The presence of $\mathbb{P}$ leads to conservation of the mean of v under the evolution. A simpler version of the argument of [1] implies that the initial value problem (1), (2) is well-posed in sufficiently regular Sobolev spaces when τ is positive; if τ were zero, then the problem would exhibit a version of the Kelvin-Helmholtz instability, and would be ill-posed.

3 The numerical method

Let $T > 0$ and $\tau > 0$ be given. Denote $\vec{u}_0 = (u_0, v_0)$. Consider a solution $\vec{u}(x,t) = (u(x,t), v(x,t))$ of (1), (2) for $x \in [0, 2\pi]$ and $t \in [0, T]$. We define the functional F by

$$F(\vec{u}_0, T) = \frac{1}{2}\int_0^{2\pi} (u(x,T) - u_0(x))^2 + (v(x,T) - v_0(x))^2\, dx. \tag{3}$$

Clearly, if the solution (u, v) is time-periodic with period T, then $F(\vec{u}_0, T) = 0$; similarly, if (u, v) is not time-periodic with period T, then $F(\vec{u}_0, T) > 0$. We therefore seek zero minimizers of the functional F.

Computationally, we use a gradient descent algorithm, the BFGS algorithm, to minimize F. In order to use this algorithm, we must be able to compute F given $\vec{u}_0$ and T, and also the derivatives $\dfrac{\delta F}{\delta \vec{u}_0}$ and $\dfrac{\delta F}{\delta T}$. We see that computation of F requires the ability to numerically solve the initial value problem; since we are using an iterative scheme, we in fact need to repeatedly solve the initial value problem. In Section 3.1, we find a formula for the necessary variational derivatives; we will see that evaluating $\dfrac{\delta F}{\delta \vec{u}_0}$ requires the numerical solution of a different, closely related initial value problem. In Section 3.2, we describe the method of solution of the initial value problems.

3.1 The variational derivative

We begin by writing the variation of F as

$$\dot{F} = \frac{d}{d\epsilon}\bigg|_{\epsilon=0} F(\vec{u}_0 + \epsilon\dot{\vec{u}}_0, T) = \int_0^{2\pi} (\vec{u}(x,T) - \vec{u}_0(x)) \cdot (\dot{\vec{u}}(x,T) - \dot{\vec{u}}_0(x))\ dx.$$

We want to write this as

$$\dot{F} = \left\langle \frac{\delta F}{\delta \vec{u}_0}, \dot{\vec{u}}_0 \right\rangle,$$

so we need to rewrite the term

$$\int_0^{2\pi} (\vec{u}(x,T) - \vec{u}_0(x)) \cdot \dot{\vec{u}}(x,T)\ dx. \tag{4}$$

To this end, we define an auxiliary quantity $\vec{Q}(x, s)$; this $\vec{Q}$ will turn out to be the solution of an evolution equation. We start by giving the initial value,

$$\vec{Q}(x, 0) = \vec{u}(x, T) - \vec{u}_0(x). \tag{5}$$

Notice that the integral (4) can then be expressed as follows:

$$\int_0^{2\pi} (\vec{u}(x,T) - \vec{u}_0(x)) \cdot \dot{\vec{u}}(x,T)\ dx = \left\langle \vec{Q}(\cdot, 0), \dot{\vec{u}}(\cdot, T) \right\rangle.$$

We would like to define $\vec{Q}$ such that for all s,

$$\left\langle \vec{Q}(\cdot, s), \dot{\vec{u}}(\cdot, T - s) \right\rangle = \left\langle \vec{Q}(\cdot, 0), \dot{\vec{u}}(\cdot, T) \right\rangle. \tag{6}$$

If we can do this, then we would have

$$\left\langle \vec{Q}(\cdot, 0), \dot{\vec{u}}(\cdot, T) \right\rangle = \left\langle \vec{Q}(\cdot, T), \dot{\vec{u}}(\cdot, 0) \right\rangle,$$

which is our desired form.

To find such a $\vec{Q}$, we differentiate (6) with respect to s :

$$\left\langle \vec{Q}_s(\cdot, s), \dot{\vec{u}}(\cdot, T - s) \right\rangle - \left\langle \vec{Q}(\cdot, s), \dot{\vec{u}}_t(\cdot, T - s) \right\rangle = 0. \tag{7}$$

If we write $\vec{u}_t = \mathbf{A}\vec{u}$, then taking the variation, we have

$$\dot{\vec{u}}_t = (D\mathbf{A}(\vec{u}))\dot{\vec{u}},$$

where $D\mathbf{A}$ is the linearization of the operator $\mathbf{A}$. If we substitute this formula into (7), then we have

$$\left\langle \vec{Q}_s(\cdot,s), \dot{\vec{u}}(\cdot,T-s) \right\rangle - \left\langle \vec{Q}(\cdot,s), (D\mathbf{A}(\vec{u}(\cdot,T-s)))\dot{\vec{u}}(\cdot,T-s) \right\rangle = 0.$$

Taking the adjoint of $D\mathbf{A}$, this is

$$\left\langle \vec{Q}_s(\cdot,s) - (D\mathbf{A}(\vec{u}(\cdot,T-s)))^* Q(\cdot,s), \dot{\vec{u}}(\cdot,T-s) \right\rangle = 0.$$

This equation will be satisfied if $\vec{Q}$ is a solution of the following evolution equation:

$$Q_s(x,s) = (D\mathbf{A}(\vec{u}(\cdot,T-s)))^* \vec{Q}(x,s). \tag{8}$$

So, (5) and (8) define an initial value problem which can be solved for $\vec{Q}$. The variational derivative of F with respect to $\vec{u}_0$ is then

$$\frac{\partial F}{\partial \vec{u}_0}(x) = \vec{Q}(x,T) - \vec{Q}(x,0).$$

We now compute $D\mathbf{A}$ and $(D\mathbf{A})^*$ for our model. Clearly, the operator $\mathbf{A}$ is given by

$$\mathbf{A}\vec{u} = \begin{bmatrix} H(v_x) \\ \tau u_{xx} + \mathbb{P}(v^2 H(u_x)) \end{bmatrix}.$$

Linearizing this, we find

$$D\mathbf{A} \begin{bmatrix} p \\ q \end{bmatrix} = \begin{bmatrix} H(q_x) \\ \tau p_{xx} + 2\mathbb{P}(vqH(u_x)) + \mathbb{P}(v^2 H(p_x)) \end{bmatrix} = \begin{bmatrix} 0 & H\partial_x \\ \tau\partial_x^2 + \mathbb{P}v^2 H\partial_x & 2\mathbb{P}vH(u_x) \end{bmatrix} \begin{bmatrix} p \\ q \end{bmatrix}.$$

The adjoint of this is

$$(D\mathbf{A})^* \begin{bmatrix} \tilde{p} \\ \tilde{q} \end{bmatrix} = \begin{bmatrix} 0 & \tau\partial_x^2 + H\partial_x v^2 \mathbb{P} \\ H\partial_x & 2vH(u_x)\mathbb{P} \end{bmatrix} \begin{bmatrix} \tilde{p} \\ \tilde{q} \end{bmatrix} = \begin{bmatrix} \tau\tilde{q}_{xx} + H\partial_x \left(v^2 \mathbb{P}\tilde{q}\right) \\ H\tilde{p}_x + 2v(\mathbb{P}\tilde{q})H(u_x) \end{bmatrix}.$$

Finally, we mention that we can compute the derivative of F with respect to T :

$$\frac{\delta F}{\delta T} = \int_0^{2\pi} (\vec{u}(x,T) - \vec{u}_0(x)) \cdot \vec{u}_t(x,T)\, dx.$$

3.2 Numerical solution of the initial value problems

Implementation of the BFGS algorithm requires accurately solving the initial value problems repeatedly; this means solving both the initial value problem for the model equations as well as for $\vec{Q}$. To do this efficiently, we use a fourth-order implicit-explicit time stepping scheme [6]. Use of this scheme allows us to remove the highest-order stiffness; instead of having a CFL condition of order 3/2, we are left with only a first-order constraint.

We compute spatial operators, i.e. spatial derivatives and Hilbert transforms, spectrally by means of the Fast Fourier Transform.

4 Time-periodic solutions of the linearized problem

There is a one-parameter family of equilibrium solutions of the model,

$$(u,v) = (0,\beta), \qquad \beta \in \mathbb{R}.$$

Fix $\beta \in \mathbb{R}$; if we linearize the model about the equilibrium, and if we denote the perturbation by $(\tilde{u}, \tilde{v})$, we have the following linearized evolution equations:

$$\tilde{u}_t = H(\tilde{v}_x), \qquad \tilde{v}_t = \tau \tilde{u}_{xx} + 2\beta^2 H(\tilde{u}_x).$$

We can rewrite this, taking the Fourier transform and writing a single second-order equation:

$$\hat{\tilde{u}}_{tt}(k,t) = \left(-\tau|k|^3 + 2\beta^2 k^2\right) \hat{\tilde{u}}(k,t). \tag{9}$$

We focus on the case in which the initial data consists of only a single non-zero mode; fix k to correspond to this mode. If $-\tau|k|^3 + 2\beta^2 k^2 < 0$, then the solutions of this problem will be periodic in time. Therefore, we assume β is such that

$$\beta^2 < \frac{\tau|k|}{2}. \tag{10}$$

If this condition is satisfied, then the solution of the problem is

$$\hat{\tilde{u}}(k,t) = \hat{\tilde{u}}(k,0) \cos\left(t\sqrt{\tau|k|^3 - 2\beta^2 k^2}\right) + \frac{\hat{\tilde{u}}_t(k,0)}{\sqrt{\tau|k|^3 - 2\beta^2 k^2}} \sin\left(t\sqrt{\tau|k|^3 - 2\beta^2 k^2}\right).$$

Inverting the Fourier transform and defining $\omega(k) = \sqrt{\tau|k|^3 - 2\beta^2 k^2}$, we have the following solutions:

$$\tilde{u}_1(x,t) = A_1 \cos(kx)\cos(\omega(k)t), \qquad \tilde{v}_1(x,t) = -\frac{A_1\omega(k)}{k} \cos(kx)\sin(\omega(k)t), \tag{11}$$

$$\tilde{u}_2(x,t) = A_2 \sin(kx)\cos(\omega(k)t), \qquad \tilde{v}_2(x,t) = -\frac{A_2\omega(k)}{k} \sin(kx)\sin(\omega(k)t), \tag{12}$$

$$\tilde{u}_3(x,t) = A_3 \cos(kx)\sin(\omega(k)t), \qquad \tilde{v}_3(x,t) = \frac{A_3\omega(k)}{k} \cos(kx)\cos(\omega(k)t), \tag{13}$$

$$\tilde{u}_4(x,t) = A_4 \sin(kx)\sin(\omega(k)t), \qquad \tilde{v}_4(x,t) = \frac{A_4\omega(k)}{k} \sin(kx)\cos(\omega(k)t). \tag{14}$$

Of course, these solutions all have temporal period

$$T = \frac{2\pi}{\omega(k)} = \frac{2\pi}{\sqrt{\tau|k|^3 - 2\beta^2 k^2}}.$$

5 Results and Discussion

We use two different methods to choose initial guesses for the BFGS algorithm when searching for time-periodic solutions of the nonlinear model. In the first method, we use the initial data for time-periodic solutions of the linearized system as initial guesses for the BFGS algorithm, with these solutions multiplied by an amplitude coefficient, δ. For instance, we could take $u = \delta\cos(x)$, $v = 0$ as the initial guess. We do this for a variety of values of δ, starting around 10^{-5}, and increasing δ incrementally until BFGS no longer returns a solution with a sufficiently small value of the functional F. We generally find that maximum values of δ for which this is effective are on the order of 10^{-1}.

The second method of generating an initial guess for the BFGS algorithm allows us to compute to higher amplitudes. In this second method, we start from previously known solutions of the nonlinear model, rather than from solutions of the linearized system. Having used the first method to generate solutions of the nonlinear model, we take the initial data from such a solution, and rescale it to have a slightly larger amplitude. This rescaled version of the initial data for a time-periodic solution becomes the initial guess for the next solution to be found; in the subsequent subsections, we describe the results from using this second method.

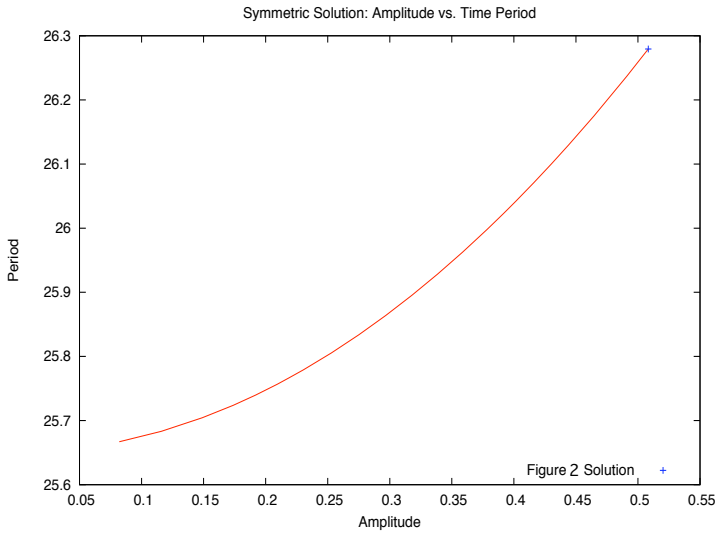

Figure 1: Amplitude of solutions versus temporal period, for solutions computed using $\tau = .06$ and $\beta = 0$. This graph was made with data from 84 different solutions.

5.1 $\beta = 0$

In Figure 1, we show the results of our computations with $\beta = 0$, as a graph of temporal period versus amplitude. We see that, combining the two methods described above for generating initial guesses for the BFGS algorithm, we are able to compute solutions of the nonlinear model, reaching amplitudes outside the linear regime. For each of the solutions represented in Figure 1, the solution has even spatial symmetry in both u and v; this is not enforced by the algorithm, but is a consequence of the original initial guess used to generate these solutions, which is $u = 0$, $v = \delta\cos(x)$ (this corresponds to the initial data for solutions of the linearization as in equation (13)). The largest-amplitude solution represented in Figure 1 is shown in detail in Figure 2. For all of these solutions, the final computed value of the functional F is 10^{-20} or smaller.

We demonstrate that it is possible to find additional solutions without such straightforward symmetries by making a different initial guess for the BFGS algorithm. By taking an initial guess of the form $u = \delta_1\cos(x)$ and $v = \delta_2\sin(x)$, we found the solution shown in Figure 3. This initial guess corresponds to a linear combination of the initial data for solutions (11) and (14) of the linearization. Notice that the amplitude for this solution is on the order of 10^{-2}; while our methods are able to find such solutions, we find that we are unable to extend these to significantly larger amplitude. For this solution, the final value of the functional F is on the order of 10^{-16}.

5.2 $\beta \neq 0$

We now consider the case of nonzero β, and for simplicity, we consider $\beta > 0$. For the value $\tau = .06$ and wavenumber $k = 1$, the restriction (10) requires

$$\beta < \sqrt{.03} \approx .1732.$$

Solutions of the model were generated using $\beta = .001$ to demonstrate that a nonzero mean may be used. With the initial guess being given a mean value for v of .001, this value was maintained throughout the

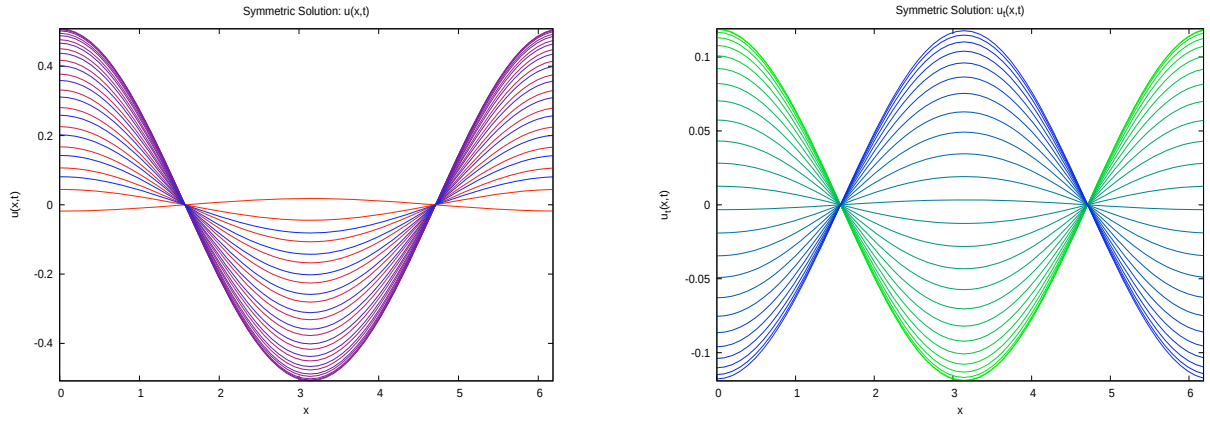

Figure 2: Profiles of a time-periodic solution of the model with $\tau = .06$ and $\beta = 0$. The left frame shows profiles of u at different times during the evolution, and the right frame shows profiles of $u_t = H(v_x)$. Note that the amplitude of u indicates that this solution cannot be considered to be in the linear regime.

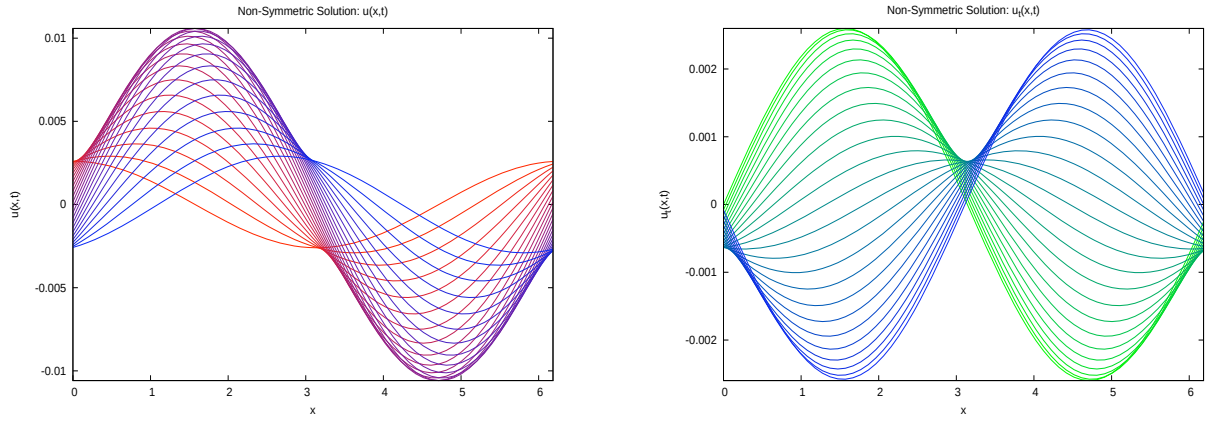

Figure 3: Profiles of a time-periodic solution of the model with $\tau = .06$ and $\beta = 0$. This solution is not either always spatially odd nor always spatially even. The left frame shows profiles of u at different times during the evolution, and the right frame shows profiles of $u_t = H(v_x)$. Note that the amplitude of u indicates that this solution is in the linear regime.

BFGS optimization process. Furthermore, the numerical continuation procedure was adapted so that each initial guess for the BFGS method had the same mean value for v; this was done by subtracting the mean, then scaling the solution, then adding the mean back to v. Results of these computations are shown as a temporal period versus amplitude graph in Figure 4. Again, for all of these solutions, the final value of the functional F is 10^{-20} or smaller.

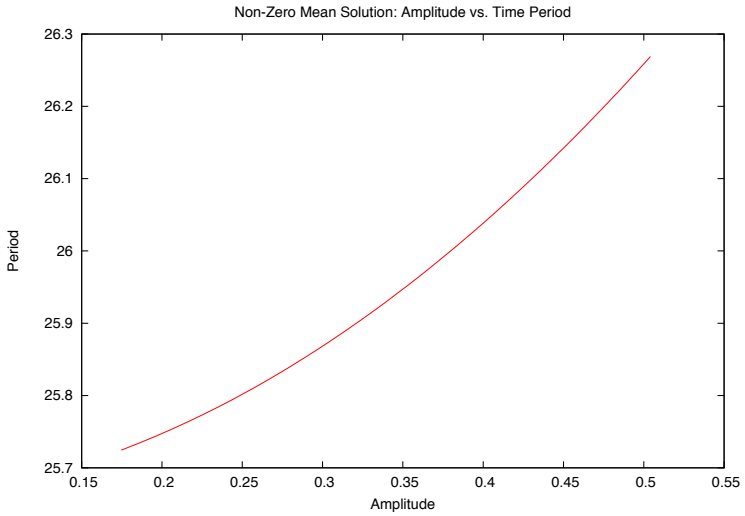

Figure 4: Amplitude of solutions versus temporal period, for solutions computed using $\tau = .06$ and $\beta = .001$. This graph was made with data from 78 different solutions.

6 Conclusion

In an earlier work, the first author put forth a model system for the vortex sheet with surface tension, and demonstrated that this model captured some of the dynamics of the problem [2]. Subsequently, the first author and Wilkening made a detailed study of the full equations of motion for the vortex sheet problem, finding a family of nontrivially time-periodic solutions bifurcating from equilibrium, attaining order-one maximum amplitude [4]. We have shown here that the model system also possesses a family of nontrivially time-periodic solutions bifurcating from equilibrium, attaining order-one maximum amplitude. This demonstrates that the features of the model (especially, a competition between dispersive effects and a destabilizing, Kelvin-Helmholtz-type nonlinearity) are sufficient to account for these dynamics, and suggests that the model system is an appropriate starting point for future studies of vortex sheet dynamics.

References

[1] David M. Ambrose. Well-posedness of vortex sheets with surface tension. *SIAM J. Math. Anal.*, 35(1):211–244 (electronic), 2003.

[2] David M. Ambrose. Singularity formation in a model for the vortex sheet with surface tension. *Math. Comput. Simulation*, 80(1):102–111, 2009.

[3] David M. Ambrose and Jon Wilkening. Global paths of time-periodic solutions of the Benjamin-Ono equation connecting pairs of traveling waves. *Commun. Appl. Math. Comput. Sci.*, 4:177–215, 2009.

[4] David M. Ambrose and Jon Wilkening. Computation of symmetric, time-periodic solutions of the vortex sheet with surface tension. *Proceedings of the National Academy of Sciences*, 107(8):3361–3366, 2010.

[5] David M. Ambrose and Jon Wilkening. Computation of time-periodic solutions of the Benjamin-Ono equation. *J. Nonlinear Sci.*, 20(3):277–308, 2010.

[6] Uri M. Ascher, Steven J. Ruuth, and Brian T. R. Wetton. Implicit-explicit methods for time-dependent partial differential equations. *SIAM J. Numer. Anal.*, 32(3):797–823, 1995.

[7] T. Brooke Benjamin and Thomas J. Bridges. Reappraisal of the Kelvin-Helmholtz problem. I. Hamiltonian structure. *J. Fluid Mech.*, 333:301–325, 1997.

[8] J. Bourgain. Construction of periodic solutions of nonlinear wave equations in higher dimension. *Geom. Funct. Anal.*, 5(4):629–639, 1995.

[9] Jean Bourgain. Construction of quasi-periodic solutions for Hamiltonian perturbations of linear equations and applications to nonlinear PDE. *Internat. Math. Res. Notices*, 1994(11):475ff., approx. 21 pp. (electronic), 1994.

[10] K. M. Case. Benjamin-Ono-related equations and their solutions. *Proc. Nat. Acad. Sci. U.S.A.*, 76(1):1–3, 1979.

[11] Walter Craig and C. Eugene Wayne. Newton's method and periodic solutions of nonlinear wave equations. *Comm. Pure Appl. Math.*, 46(11):1409–1498, 1993.

[12] F. de la Hoz, M. A. Fontelos, and L. Vega. The effect of surface tension on the Moore singularity of vortex sheet dynamics. *J. Nonlinear Sci.*, 18(4):463–484, 2008.

[13] T. Y. Hou, J. S. Lowengrub, and M. J. Shelley. The long-time motion of vortex sheets with surface tension. *Phys. Fluids*, 9(7):1933–1954, 1997.

[14] Thomas Y. Hou, John S. Lowengrub, and Michael J. Shelley. Removing the stiffness from interfacial flows with surface tension. *J. Comput. Phys.*, 114(2):312–338, 1994.

[15] G. Iooss, P. I. Plotnikov, and J. F. Toland. Standing waves on an infinitely deep perfect fluid under gravity. *Arch. Ration. Mech. Anal.*, 177(3):367–478, 2005.

[16] Robert Krasny. A study of singularity formation in a vortex sheet by the point-vortex approximation. *J. Fluid Mech.*, 167:65–93, 1986.

[17] D. W. Moore. The spontaneous appearance of a singularity in the shape of an evolving vortex sheet. *Proc. Roy. Soc. London Ser. A*, 365(1720):105–119, 1979.

[18] Jorge Nocedal and Stephen J. Wright. *Numerical optimization*. Springer Series in Operations Research and Financial Engineering. Springer, New York, second edition, 2006.

[19] P. I. Plotnikov and J. F. Toland. Nash-Moser theory for standing water waves. *Arch. Ration. Mech. Anal.*, 159(1):1–83, 2001.

[20] M. J. Shelley. A study of singularity formation in vortex-sheet motion by a spectrally accurate vortex method. *J. Fluid Mech.*, 244:493–526, 1992.

[21] Michael Siegel. A study of singularity formation in the Kelvin-Helmholtz instability with surface tension. *SIAM J. Appl. Math.*, 55(4):865–891, 1995.

[22] Jon Wilkening. Breakdown of self-similarity at the crests of large-amplitude standing water waves. *Phys. Rev. Lett.*, 107:184501, Oct 2011.

[23] V. E. Zakharov. Stability of periodic waves of finite amplitude on the surface of a deep fluid. *Journal of Applied Mechanics and Technical Physics*, 9:190–194, 1968.